Exciplex and excimer molecular probes: detection of conformational flip in a *myo*-inositol chair†

Manikandan Kadirvel, Biljana Arsic, Sally Freeman* and Elena V. Bichenkova*

Received 15th January 2008, Accepted 3rd March 2008
First published as an Advance Article on the web 9th April 2008
DOI: 10.1039/b800710a

2-*O*-*tert*-Butyldimethylsilyl-4,6-bis-*O*-pyrenoyl-*myo*-inositol-1,3,5-orthoformate (**6**) and 2-*O*-*tert*-butyldimethylsilyl-4-*O*-[4-(dimethylamino)benzoyl]-6-*O*-pyrenoyl-*myo*-inositol-1,3,5-orthoacetate (**10**) adopt conformationally restricted unstable chairs with five axial substituents. In the symmetrical diester **6**, the two π-stacked pyrenoyl groups are electron acceptor–donor partners, giving a strong intramolecular excimer emission. In the mixed ester **10**, the pyrenoyl group is the electron acceptor and the 4-(dimethylamino)benzoyl ester is the electron donor, giving a strong intramolecular exciplex emission. The conformation of the mixed ester **10** was assessed using ^{1}H NMR spectroscopy (^{1}H-NOESY) and computational studies. which showed the minimum inter-centroid distance between the two aromatic systems to be ~3.9 Å. Upon addition of acid, the orthoformate/orthoacetate trigger in **6**and **10** was cleaved, which caused a switch of the conformation of the *myo*-inositol ring to the more stable penta-equatorial chair, leading to separation of the aromatic ester groups and loss of excimer and exciplex fluorescence, respectively. This study provides proof of principle for the development of novel fluorescent molecular probes.

Introduction

Exciplex- and excimer-based molecular probes[1–4] offer a number of advantages over common detection approaches, which utilise conventional fluorescence dyes as reporter groups. On correct three-dimensional alignment of exci-partners, these probes can produce specific fluorescence emission at much longer wavelengths than individual fluorescence partners separated in space by more than ~4 Å. This means that the colour of the fully assembled excimer or exciplex detector is visibly different to that of the individual components, and thus direct visualisation approaches may be possible for detection.

Another advantage of excimer- and exciplex-based detection approaches is substantially reduced background fluorescence at the detection wavelength.[1–4] Earlier, excimer-based oligonucleotide molecular probes have been reported for the detection of nucleic acids.[5–9] Recently, we developed an alternative approach based on an exciplex detector:[1–4] oligonucleotide split-probes (exciprobes) equipped with the exciplex partners were shown to be capable of emitting characteristic exciplex fluorescence (at ~480 nm) on correct self-assembly by their bio-target. Exciprobes were also assessed for their ability to detect certain nucleic acid sequences and discriminate mutations at the level of PCR products and plasmid DNA molecules.[4]

An exceptional sensitivity of excimer or exciplex detectors to the spatial separation between the exci-partners makes it possible to monitor fine conformational re-arrangements within molecules. These unique properties can be used, for example, to develop novel molecular probes capable of signalling the presence of certain chemical or biological factors (*e.g.* high cellular levels of H^+, metal ions or certain enzymes). Here we propose a simple concept to monitor conformational ring-flip of a *myo*-inositol cyclohexane chair using excimer and exciplex molecular detectors. *myo*-Inositol has five equatorial hydroxy groups in its most stable chair conformation. The 1,3,5-orthoformate or 1,3,5-orthoacetate of *myo*-inositol locks the chair in the unstable penta-axial conformation by simultaneously protecting the *cis*-1,3,5-trihydroxy groups.[10,11] This protecting group was chosen to exploit the acid-labile nature of orthoesters, which leads to an acid-sensitive conformational trigger, a potentially useful tool to monitor an elevated level of H^+ in physiologically abnormal tissues. In 2-*O*-*tert*-butyldimethylsilyl-4,6-bis-*O*-pyrenoyl-*myo*-inositol-1,3,5-orthoformate (**6**), two closely located π-stacked pyrenoyl fluorescent groups form an excimer (an excited state dimer) on specific excitation at 335 nm. In the mixed ester 2-*O*-*tert*-butyldimethylsilyl-4-*O*-[4-(dimethylamino)benzoyl]-6-*O*-pyrenoyl-*myo*-inositol-1,3,5- orthoacetate (**10**), the 4-(dimethylamino)benzoyl (electron donor) and pyrenoyl (electron acceptor) groups form an exciplex (excited state complex) on pyrene excitation at 335 nm. An acid-induced cleavage of orthoformate or orthoacetate trigger in **6** and **10**, respectively, switches the conformationally locked penta-axial *myo*-inositol ring to the more stable penta-equatorial chair conformation, which is accompanied by a loss of interaction between the donor/acceptor aromatic partners with subsequent disappearance of the excimer or exciplex fluorescence band. A preliminary account of this research has been published.[12]

Results and discussion

Synthesis of *myo*-inositol-pyrene-based derivatives

myo-Inositol-1,3,5-orthoformate **2** and *myo*-inositol-1,3,5-orthoacetate **3** were prepared by the reaction of *myo*-inositol **1**

School of Pharmacy and Pharmaceutical Sciences, The University of Manchester, Oxford Road, Manchester, M13 9PT, UK. E-mail: sally.freeman@manchester.ac.uk, Elena.V.Bichenkova@manchester.ac.uk

† Electronic supplementary information (ESI) available: NMR spectra. See DOI: 10.1039/b800710a

with triethyl orthoformate or triethyl orthoacetate, respectively, in the presence of acid catalyst.[10,11] The 2-equatorial hydroxyl groups were protected using *tert*-butyldimethylsilyl chloride to give the diols **4** and **5** (Schemes 1 and 2).[13] The bispyrenoyl excimer **6** was prepared in 48% yield by esterification of the 4,6-diaxial hydroxyl groups of **4** using pyrene-1-carboxylic acid, DCC and DMAP[14] in equal proportions, with the monopyrenoyl ester **7** being isolated as a by-product in 16% yield (Scheme 1). Attempts to promote the formation of bispyrenoyl ester **6** with a larger excess of coupling reagents led to the formation of an unwanted amide, *N*-acylurea, formed due to slow acyl migration.[15] Acidic esterification conditions were avoided so as to minimise the decomposition of the orthoformate/orthoacetate moiety (Scheme 1). The adopted coupling procedure using DCC and DMAP was an effective method for the esterification of sterically demanding, acid-labile substrates.[14,16]

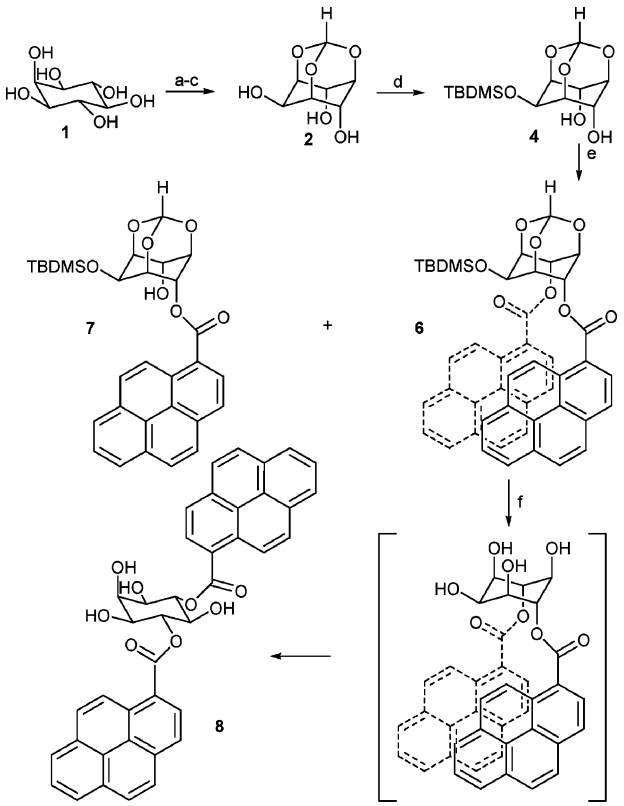

Scheme 1 Synthesis of excimer **6** and deprotection to **8**. *Reagents and conditions*: (a) triethyl orthoformate, *p*-TsOH, dry DMF; (b) benzoyl chloride, dry pyridine; (c) isobutylamine, methanol; (d) TBDMSCl, 2,6-lutidine, dry DMF; (e) pyrene-1-carboxylic acid, DCC, DMAP, dry DCM; (f) 80% TFA–water.

The mixed diester **10** was prepared by reaction of diol **5** with donor 4-(dimethylamino)benzoic acid in the presence of DCC to give monoester **9** (Scheme 2). The first esterification of the diol proceeded well, due to the high acidity of the hydrogen-bonded OH in diol **5**.[15,17] The reaction of the monoester **9** with the less reactive pyrene-1-carboxylic acid (Scheme 2) under the DCC/DMAP coupling conditions[14,16] gave **10** in a yield of 50%.

Hydrolysis and release of the 1,3,5-orthoformate or 1,3,5-orthoacetate conformational lock was achieved by acid-catalysed

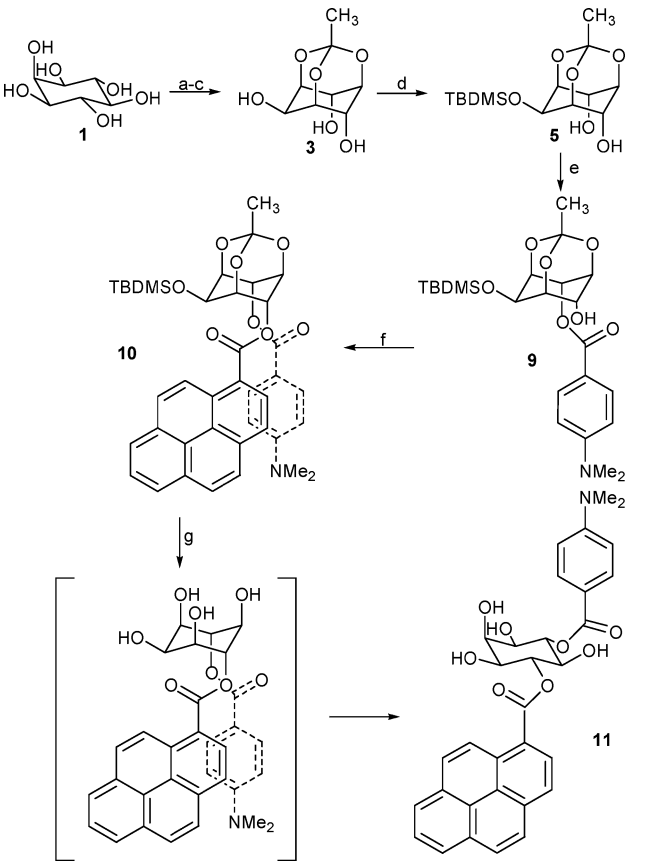

Scheme 2 Synthesis of exciplex **10** and deprotection to **11**. *Reagents and conditions*: (a) triethyl orthoacetate, *p*-TsOH, dry DMF; (b) benzoyl chloride, dry pyridine; (c) isobutylamine, methanol; (d) TBDMSCl, 2,6-lutidine, dry DMF; (e) 4-(dimethylamino)benzoic acid, DCC, DMAP, dry DCM; (f) pyrene-1-carboxylic acid, DCC, DMAP, dry DCM; (g) 80% TFA–water.

hydrolysis.[18,19] The bispyrenoyl ester **6** and mixed pyrenoyl 4-(dimethylamino)benzoyl ester **10** were treated with 80% trifluoroacetic acid in water[13] to give **8** and **11**, respectively (Schemes 1 and 2). The orthoacetate group cleaves to give the acetyl ester first, with subsequent hydrolysis to acetic acid.[20] Besides cleavage of the orthoformate/orthoacetate groups, the *tert*-butyldimethylsilyl groups of **6** and **10** were also cleaved. ^{1}H NMR monitoring of the hydrolysis of orthoacetate **10** by 80% TFA in D_2O at 25 °C showed that after 5 min the orthoacetate unit had cleaved, with subsequent conformational change of the constrained penta-axial orthoester **10** to the more stable penta-equatorial chair **11**. The 4-(dimethylamino)benzoyl and pyrenoyl esters were largely intact after 38 h; however, a small amount of ester hydrolysis occurred over time. Novel compounds **5–11** were fully characterised by ^{1}H and ^{13}C NMR spectroscopy, mass spectrometry and elemental analysis.

NMR and fluorescence analysis

Proton signal assignments for compounds **5–11** were achieved using 1D NMR and ^{1}H COSY. The results of proton assignments for **5–11** are presented in the Experimental section and described in the ESI.† Chemical shifts and coupling constants for some

Table 1 Chemical shifts (in ppm) and spin–spin coupling constants (in Hz) for selected protons within compounds **6–11**

Compound	Ins H-4	Pyr H-8	Pyr H-16	NMe_2	Ar H-17	Ar H-18
Bis-pyrenoyl analogue (**6**)	δ 5.94 (t), $J = 3.8$	δ 8.74 (d), $J = 9.4$	δ 7.93 (d), $J = 8.4$	—	—	—
Mono-pyrenoyl analogue (**7**)	δ 5.93–5.97 (m)	δ 9.26 (d), $J = 9.4$	δ 8.55 (d), $J = 8.1$	—	—	—
Deprotected analogue (**8**)	δ 5.66 (t), $J = 9.9$	δ 9.11 (d), $J = 9.6$	δ 8.66 (d), $J = 8.1$	—	—	—
4-(Dimethylamino)benzoyl monomer (**9**)	δ 5.70–5.74 (m)	—	—	δ 3.05 (s)	δ 7.79 (d), $J = 8.8$	δ 6.63 (d), $J = 9.0$
Pyrenoyl-4-(dimethylamino)-benzoyl ester (**10**)	δ 5.67 (t), $J = 9.4$	δ 8.89 (d), $J = 9.4$	δ 8.34 (d), $J = 8.1$	δ 2.16 (s)	δ 7.15 (d), $J = 9.3$	δ 5.30 (d), $J = 9.1$
Deprotected analogue (**11**)	δ 5.64 (t), $J = 9.7$	δ 9.26 (d), $J = 9.4$	δ 8.70 (d), $J = 8.1$	δ 3.03 (s)	δ 7.91 (d), $J = 9.2$	δ 6.71 (d), $J = 9.2$

selected protons in compounds **6–11** are shown in Table 1. The numbering of protons is shown in Scheme 3.

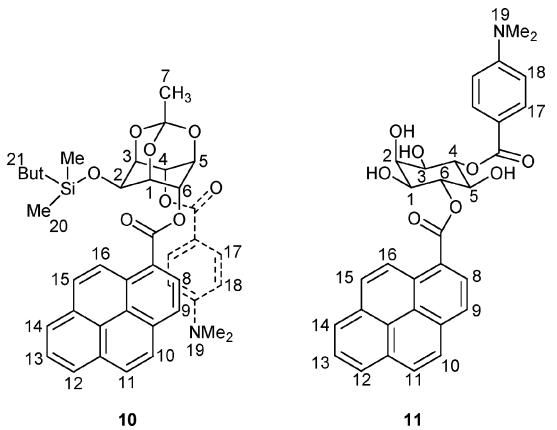

Scheme 3 Numbering of protons of analogues **10** and **11** used for ^{1}H NMR signal assignment.

In the ^{1}H NMR spectrum, some aromatic protons of the bispyrenoyl analogue **6** and mixed ester **10** showed substantial upfield shifts (see Table 1) compared with the respective monoester analogues **7** and **9**, presumably due to π-stacking interactions between aromatic rings in **6** and **10**. For example, protons H-17, H-18 and -N$(CH_3)_2$ (H-19) of DMAB (see Scheme 3 for proton numbering) within **10** showed upfield shifts of 0.64, 1.33 and 0.89 ppm, respectively, compared to those in **9**. Pyrenoyl protons H-8 and H-16 within **10** were shifted to higher field by 0.37 and 0.21 ppm, respectively, compared to those in **7**. The upfield shifts of pyrenoyl protons within the bispyrenoyl analogue **6** were even more pronounced: protons H-8 and H-16 showed upfield shifts of 0.52 and 0.62 ppm, respectively, compared to those in **7**, indicating strong π-stacking interactions between closely located pyrenoyl rings within **6**. The inositol proton (H-4) of **6** and **10** gave triplets with small J_{eq-eq} coupling constants of 3.8 Hz, consistent with a penta-axial chair conformation (Table 1).

Fluorescence studies also supported close spatial location of exci-partners within **6** and **10**, showing the formation of excimer and exciplex, respectively. Emission spectra of the compounds were recorded at a low concentration (1×10^{-5} M) in chloroform to avoid any intermolecular interactions (Fig. 1). The emission spectra of **6** and **10** showed characteristic bands attributed to the locally excited state of the pyrene monomer with emission λ_{max} at 386 nm and 396 nm for the analogues **6** and **10**, respectively. In addition, excimer and exciplex emissions were observed for compounds **6** and **10** with green fluorescence at 524 nm and 520 nm, respectively. The intensity of the excimer fluorescence emission for **6** was higher than the exciplex emission for **10**. These fluorescence studies demonstrated that an excimer or exciplex can be formed in the ring-constrained penta-axial conformation of *myo*-inositol due to the close proximity of the reporter groups.

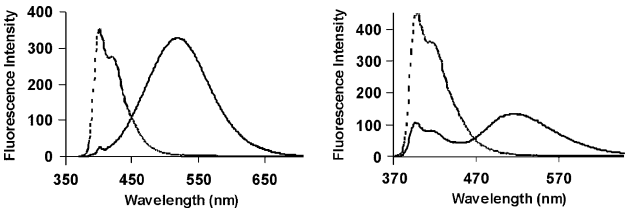

Fig. 1 Left: Emission spectra of 2-*O*-*tert*-butyldimethylsilyl-4,6-bis-*O*-pyrenoyl-*myo*-inositol-1,3,5-orthoformate (**6**; solid) and its deprotected analogue, 4,6-bis-*O*-pyrenoyl-*myo*-inositol (**8**; dashed). Right: Emission spectra of 2-*O*-*tert*-butyldimethylsilyl-4-*O*-[4-(dimethylamino)-benzoyl]-6-*O*-pyrenoyl-*myo*-inositol-1,3,5-orthoformate (**10**; solid) and its deprotected analogue 4-*O*-[4-(dimethylamino)benzoyl]-6-*O*-pyrenoyl-*myo*-inositol (**11**; dashed). Spectra were recorded at a concentration of 1×10^{-5} M in chloroform at 20 °C. Excitation and emission slit widths were 3 nm for 6 and 10, and 1.5 nm for 8 and 11.

Fluorescence experiments monitoring the conformational change induced by acid deprotection of the orthoacetate/orthoformate groups in **6** and **10** to give **8** and **11**, respectively, showed the disappearance of the excimer and exciplex emission seen for **6** and **10**, with the observation of blue fluorescence at 386 nm attributed to a locally excited state of the pyrene monomer (Fig. 1). The excitation spectrum of **8** showed a strong blue shift (*ca.* 43 nm) of the major excitation band compared to that for the protected analogue **6**. This shift is presumably attributed to disappearance of π–π stacking interactions of the two pyrenoyl moieties in the ground state of **8**. In addition, there was a significant downfield shift of the aromatic protons in the ^{1}H NMR spectrum of **8** and **11** compared with **6** and **10**, respectively, confirming loss of π–π stacking in the deprotected analogues (see Table 1). Inositol H-4 triplets, with J_{ax-ax} values of 9.9 Hz for **8** and 9.7 Hz for **11**, were also consistent with the more stable penta-equatorial ring-flipped chair conformation (Table 1).

Table 2 Inter-proton distances between the two aromatic systems and inositol moiety and aromatic system calculated for conformers **10a**, **10b** and **10c** in $CHCl_3$ along with the respective relative intensities of cross-peaks, observed in the ^1H NOESY spectrum ($CDCl_3$)

	Inter-proton distances/Å				
Intramolecular contacts	**10a**	**10b**	**10c**	Cross-peak assignment (coordinate/ppm)	Relative intensity of observed NOESY cross-peak[a]
DMAB (H-17)–Ins (H-2)	2.89	3.16	***2.40***	**1** (7.00–4.30)	M
Pyr (H-8)–Ins (H-5)	4.26	3.90	***3.68***	**2** (8.70–4.85)	V
Pyr (H-16)–Ins (H-2)	2.76	***4.73***	***3.93***	**3** (8.70–4.35)	M
Pyr (H-8)–Ins (H-2)	5.16	5.60	5.58	**4** (8.34–4.35)	V
Pyr (H-9)–$N(CH_3)_2$ (H-19)	3.00	***7.44***	3.19	**5** (8.10–1.92)	S
Pyr (H-16)–DMAB (H-17)	3.40	2.84	3.29	**6** (8.15–7.00)	S
Pyr (H-15)–DMAB (H-18)	3.67	***6.43***	3.91	**7** (7.80–5.10)	V
CH_3 (H-21)–DMAB (H-17)	3.68	3.55	***4.92***	**8** (1.40–7.00)	V
CH_3 (H-21)–Pyr (H-16)	3.88	***6.81***	***6.91***	**9** (1.40–8.15)	V

[a] Relative intensities of observed cross-peaks for proton–proton interactions are ranked as very small (V), small (S), medium (M) and large (L) corresponding to $3.5 \leq r \leq 5.0$ Å, $2.5 \leq r \leq 3.5$ Å, $2.3 \leq r \leq 2.8$ Å and $1.0 \leq r \leq 1.9$ Å, respectively. The relative intensities for methyl group (centered at the carbon of the methyl group) proton–proton interactions are $3.5 \leq r \leq 5.5$ Å, $2.5 \leq r \leq 4.0$ Å, $2.3 \leq r \leq 3.3$ Å and $1.0 \leq r \leq 2.4$ Å, respectively.[22] Peak intensities are classified relative to reference cross-peak **A**, reflecting DMAB (H-17)–DMAB (H-18) intra-residue interactions (2.45 Å).

2D NMR spectroscopic analysis of the ground state conformation of 10

The ^1H NOESY spectrum of **10** is provided in the ESI†, and demonstrates that the aromatic rings of the exciplex partners are in close spatial proximity, which allows π–π-stacking interactions. This is in agreement with the substantial upfield shifts observed for some aromatic protons of **10** (see above) compared to those of the mono-substituted derivatives **7** and **9** (Table 1). Analysis of the ^1H NOESY spectrum revealed a number of inter-residue NOE interactions (positive cross-peaks **1–9**) between DMAB, pyrenoyl and inositol moieties, as summarised in Table 2 and discussed in the ESI†. This provided evidence of close spatial proximity of the 4-(dimethylamino)benzoyl (an electron donor) and pyrenoyl (an electron acceptor) groups within the conformationally restricted unstable chair conformation locked by the 1,3,5-orthoacetate protecting group. Relative intensities of observed NOESY inter-residue cross-peaks were used to estimate distance ranges for interacting protons of the 4-(dimethylamino)benzoyl and pyrenoyl groups[21] (see Table 2). Cross-peak **A**, reflecting intra-residue interactions between DMAB (H-17) and DMAB (H-18) protons (with a distance of 2.45 Å between them), was used as a reference peak.

Pyr (H-16), and especially Pyr (H-8), protons were found to be the most downfield signals, reflecting the influence from the closely located carbonyl group. Signals of Pyr (H-9) and Pyr (H-15) were assigned *via* their interactions with Pyr (H-8) and Pyr (H-16), respectively. The assignment of the individual pyrene protons Pyr (H-10)–Pyr (H-14) was not possible due to extensive overlapping of these signals in the aromatic region of 7.5–8.2 ppm and due to close location of the respective cross-peaks to the diagonal in the COSY and NOESY spectra.

Computational conformational analysis. Conformational analysis of **10** was performed using molecular dynamics (Sybyl 7.3, Tripos Associates).[22] Annealed structures were energy-minimized using the Tripos[23] force field. Three low energy conformers for exciplex **10** are presented in Fig. 2.

The conformer **10a** (Fig. 2) with lowest energy (E= −1.146 kcal mol^{-1}) had a distance between the centroids of the donor and acceptor groups of 4.34 Å. The second most stable conformation, with a significantly higher energy (E = 6.799 kcal mol^{-1}) (**10b**) gave a longer distance between the centroids of 8.10 Å. The third most favourable conformer, with an energy of E = 6.917 kcal mol^{-1}, had a distance of 3.97 Å between the centroids.

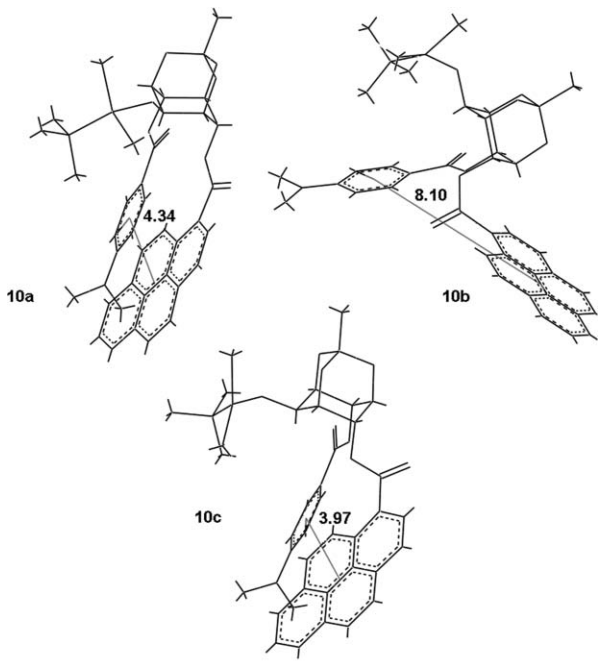

Fig. 2 Three minimum energy conformations of **10** calculated using the Tripos force field. Inter-centroid distances between the aromatic rings of the exci-partners are given in Å.

Correlation between NMR and molecular modelling data. Table 2 represents some proton–proton distances calculated for conformers **10a**, **10b** and **10c** in chloroform, together with the respective relative intensities of cross-peaks, observed in the ^1H NOESY spectrum recorded in $CDCl_3$.

It can be seen that distances calculated for conformation **10a** (the lowest energy structure) entirely satisfied experimental NOE

observations, suggesting that this structure could represent the average conformation of **10** in solution. Distances calculated for conformation **10b** show some correlation with the experimental data; however, there are four interactions (Pyr (H-15)–DMAB (H-18); Pyr (H-16)–Ins (H-2); Pyr(H-9)–$N(CH_3)_2$ (H-19); CH_3 (H-21)–Pyr (H-16), shown in ***bold italics***), which do not match experimental data. Structure **10c** showed some correlation with experimental NOESY NMR data (Table 2). The discrepancies shown in ***bold italics*** are: DMAB (H-17)–Ins (H-2); Pyr (H-8)–Ins (H-5); CH_3 (H-21)–DMAB (H-17); CH_3 (H-21)–Pyr (H-16). The solution structure could be a combination of **10a** (major) and **10b** and **10c** (minor) conformers.

2D NMR spectroscopic analysis of ground state conformation of 11

Analysis of the ^{1}H NOESY spectrum of deprotected compound **11** revealed cross-peaks corresponding to the intra-residue interactions within the pyrenoyl moiety, the 4-(dimethylamino)benzoyl group and the inositol ring as summarized in the ESI†. The NOESY spectrum of **11** showed that there were no through-space interactions between the 4-(dimethylamino)benzoyl and 6-pyrenoyl groups for this deprotected analogue, consistent with the more stable penta-equatorial ring-flipped chair conformation. All inter-residue NOE interactions between the exciplex partners seen for **10** disappeared for its deprotected analogue **11**, indicating spatial separation of DMAB and pyrenoyl groups after deprotection.

Computational studies also showed substantial separation between the exciplex partners as well as a higher degree of conformational freedom for structure **11**. A number of low-energy conformations were found for **11**, which were close in energy with the distance between the centroids of the aromatic systems ranging from 11.1 Å to 13.0 Å (Fig. 3 as an example).

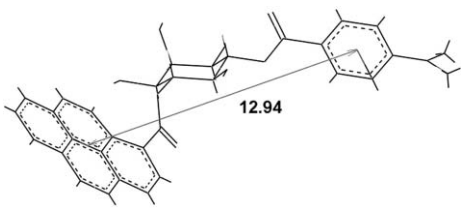

Fig. 3 One low-energy conformer of structure **11** obtained from conformational analysis using the Tripos force field in chloroform. The inter-centroid distance for the conformer is given in Å.

Conclusions

Excimer and exciplex formation has been used to monitor conformational change during the ring-flip of a *myo*-inositol cyclohexane chair. Dramatic changes in the fluorescence and NMR spectra are consistent with the penta-axial conformation of **6** and **10** undergoing an ring flip caused by acid-induced hydrolysis of orthoformate/orthoacetate trigger to the energetically preferred penta-equatorial conformation of **8** and **11** (Schemes 1 and 2). This is the first example where excimer and exciplex fluorescence has been used to monitor the triggering of a conformationally locked cyclohexane ring (with an minimum inter-centroid distance between the reporter groups of ~3.9 Å) to the more stable penta-equatorial chair conformation (with an inter-centroid distance between the reporter groups of ~11–12.9 Å). Complete loss of excimer and exciplex fluorescence was observed for compounds **6** and **10**, respectively, upon acid-triggered conformational change. 2D NMR spectroscopy (^{1}H NOESY) and molecular modelling gave the structural explanations of the obtained fluorescence observations, providing necessary background for further development of inositol-based molecular detectors. Studies are in progress towards the development of novel fluorescent molecular probes for detection of certain chemical or biological factors, for example high cellular levels of H^+ in vacuoles in cells and hypoxic tumour cells, metal ions or certain enzymes.

Experimental

Materials and methods

Chemicals were purchased from Aldrich Chemical Co., Gillingham, UK. Syntheses were monitored by thin layer chromatography on pre-coated 60 F_{254} silica gel aluminium-backed plates (Merck, Darmstadt). Visualisation of spots for thin layer chromatography was performed using a UV GL-58 Mineral-Light lamp. Melting points were determined using a Gallenkamp Melting Point apparatus microscope (UK). IR spectra were recorded using a Bruker Tensor 27 spectrometer (resolution 4 cm^{-1}). NMR spectra were recorded using a Bruker Avance-300 spectrometer (7.05 T) equipped with a 5 mm single-axis Z-gradient quattro nucleus probe, operating at 300 MHz for ^{1}H and at 75 MHz for ^{13}C. The spectrometer was operated using XWIN NMR system software. Chemical shifts (δ) are reported in parts per million (ppm), with peak positions relative to Me_4Si (0.00 ppm) as internal reference. Abbreviations used for splitting patterns are: s, singlet; d, doublet; t, triplet; m, unresolved multiplet. Mass spectra were recorded at the School of Chemistry, University of Manchester, using a Micromass PLATFORM II (ES and APCI) and Thermo Finnigan MAT95XP (accurate mass) instrument. Elemental analyses were recorded in the School of Chemistry, University of Manchester, using an EA 1108 Elemental Analyzer (Carlo Erba Instruments).

Synthesis

2-*O*-*tert*-Butyldimethylsilyl-*myo*-inositol-1,3,5-orthoacetate (5). A mixture of *myo*-inositol-1,3,5-orthoacetate **3** (3.0 g, 0.0147 mol), *tert*-butyldimethylsilyl chloride (2.3 g, 0.0148 mol) and 2,6-lutidine (4.5 mL, 0.0382 mol) was suspended in dry DMF (30 mL) and stirred at room temperature for 48 h. A white turbid mass was observed after 30 min. The reaction mixture was filtered and the filtrate was concentrated under reduced pressure to remove DMF. The resultant gum was diluted with cold water (30 mL) and stirred at room temperature for 4 h. The colourless solid was filtered and dried to give 3.0 g (65%) of **5**. Mp 242–245 °C; ^{1}H NMR ($CDCl_3$) δ 4.55 (2H, t, J 3.8 Hz, H-4,6), 4.18–4.21 (2H, m, H-2,5), 4.15–4.16 (2H, m, H-1,3), 1.47 (3H, s, CH_3 H-7), 0.95 (9H, s, Bu^t), 0.15 (6H, s, $SiMe_2$). ^{13}C NMR ($CDCl_3$) δ 108.1 (C-7), 75.2 (C-1,3), 69.0 (C-5), 68.5 (C-4,6), 59.5 (C-2), 25.5 (CMe_3), 24.2 (Me), 18.4 (CMe_3), −5.1 ($SiMe_2$). MS (electrospray) m/z $[M + Cl]^-$ 353.1. Accurate mass calcd for $C_{14}H_{26}O_6ClSi$: 353.1193: Found 353.1196.

2-*O*-*tert*-Butyldimethylsilyl-4,6-bis-*O*-pyrenoyl-*myo*-inositol-1,3,5-orthoformate (6) and 2-*O*-*tert*-butyldimethylsilyl-4-*O*-pyrenoyl-*myo*-inositol-1,3,5-orthoformate (7). DCC (0.69 g, 3.4 mmol) and DMAP (0.05 g, 0.16 mmol) were added to a solution of pyrene-1-carboxylic acid (1.0 g, 4.1 mmol) in dry DCM (20 mL). The mixture was stirred at room temperature under a nitrogen atmosphere. 2-O-*tert*-Butyldimethylsilyl-*myo*-inositol-1,3,5-orthoformate (**4**) (0.50 g, 1.6 mmol) was added to the above solution and the mixture was stirred at room temperature for 24 h. Completion of the reaction was monitored by TLC, R_f 0.64 (hexane–EtOAc 3 : 1). The reaction mixture was filtered and the filtrate concentrated under reduced pressure. The residue was purified by flash column chromatography (hexane–EtOAc 3 : 1) to give 0.60 g (48%) of **6**. Mp 262–265 °C. IR ν 1718 (C=O) cm^{-1}. ^1H NMR ($CDCl_3$) (assignments using ^1H COSY) δ 8.74 (2H, d, J 9.4 Hz, Pyr H-8), 7.93 (2H, d, J 8.4 Hz, Pyr H-16), 7.88–7.12 (14H, m, Pyr H-9–H-15), 5.94 (2H, t, J 3.8 Hz, H-4,6), 5.80 (1H, d, $^5J_{7\text{-}2}$ 1.1 Hz, CH-7), 5.40–5.44 (1H, m, H-5), 4.70–4.73 (1H, m, H-2), 4.51–4.53 (2H, m, H-1,3), 1.09 (9H, s, Bu^t), 0.33 (6H, s, $SiMe_2$). ^{13}C NMR ($CDCl_3$) δ 165.8 (C=O), 133.8, 130.8, 130.1, 129.4, 129.1, 127.3, 126.0, 125.8, 125.7, 124.5, 123.7, 123.5, 122.8, 122.7, 120.8 (Pyr-C), 103.4 (C-7), 76.5 (C-4,6), 72.4 (C-5), 69.1 (C-2), 66.0 (C-1,3), 26.1 (CMe_3), 18.7 (CMe_3), −4.5 ($SiMe_2$). MS (APCI) m/z $[M + H]^+$ 761.0. Anal. Calcd for $C_{47}H_{40}O_8Si$: C, 74.19; H, 5.30. Found C, 73.83; H, 5.21%. Compound **7** (0.14 g, 16%) was also isolated. Mp 218–221 °C. IR ν 3491(O–H), 1710 (C=O) cm^{-1}. ^1H NMR ($CDCl_3$) (assignments using COSY) δ 9.26 (1H, d, J 9.4 Hz, Pyr H-8), 8.55 (1H, d, J 8.1 Hz, Pyr H-16), 8.07–8.32 (7H, m, Pyr H-9-H-15), 5.93–5.97 (1H, m, H-4), 5.80 (1H, d, $^5J_{7\text{-}2}$ 1.1 Hz, CH-7), 4.72–4.74 (1H, m, H-5), 4.66–4.68 (1H, m, H-2), 4.49–5.01 (1H, m, H-1), 4.44–4.46 (1H, m, H-3), 4.50–4.52 (1H, m, H-6), 0.95 (9H, s, Bu^t), 0.18 (6H, s, $SiMe_2$). ^{13}C NMR ($CDCl_3$) δ 165.9 (C=O), 134.9, 131.6, 131.0, 130.3, 130.2, 130.0, 128.1, 127.0, 126.7, 126.6, 124.9, 124.8, 122.4, 124.2, 124.0, 121.7 (Pyr-C), 103.0 (C-7), 74.6 (C-4), 72.4 (C-5), 69.6 (C-2), 68.6 (C-1), 68.0 (C-3), 61.3 (C-6), 25.9 (CMe_3), 18.5 (CMe_3), −4.6 ($SiMe_2$). MS (APCI) m/z $[M + H]^+$ 533.0. Anal. calcd for $C_{30}H_{32}O_7Si.0.5H_2O$: C, 66.52; H, 6.15. Found C, 66.41; H, 5.72%.

2-*O*-*tert*-Butyldimethylsilyl-4-*O*-[4-(dimethylamino)benzoyl]-*myo*-inositol-1,3,5-orthoacetate (9). DCC (0.72 g, 3.5 mmol) and DMAP (0.1 g, 0.3 mmol) were added to a solution of 4-(dimethylamino)benzoic acid (0.58 g, 3.5 mmol) in 20 mL of dry DCM at room temperature under a nitrogen atmosphere. 2-O-*tert*-Butyldimethylsilyl-*myo*-inositol-1,3,5-orthoacetate (**5**) (1.0 g, 3.1 mmol) was added and the reaction mixture was stirred at room temperature for 24 h. The reaction mass was filtered, and the filtrate concentrated under reduced pressure. The residue was purified by flash column chromatography (hexane–EtOAc 3 : 1) to give 0.91 g (62%) of **9**. Mp 258–261 °C. IR ν 3491(O–H), 1710 (C=O) cm^{-1}. ^1H NMR ($CDCl_3$) δ 7.79 (2H, d, J 8.8 Hz, Ar H-17), 6.63 (2H, d, J 9.0 Hz, Ar H-18), 5.70–5.74 (1H, m, H-4), 4.53–4.55 (1H, m, H-5), 4.36–4.38 (2H, m, H-2), 4.27–4.29 (1H, m, H-1,3), 4.16–4.18 (1H, m, H-6), 3.05 (6H, s, NMe_2), 1.50 (3H, s, CH_3 H-7), 0.93 (9H, s, Bu^t), 0.13 (6H, s, $SiMe_2$). ^{13}C NMR ($CDCl_3$) δ 164.9 (C=O), 153.7 (Ar C-4), 131.6 (Ar C-2,6), 115.0 (Ar C-1), 111.0 (Ar C-3,5), 108.7 (C-7), 76.6 (C-4), 75.3 (C-5), 73.0 (C-2), 68.6 (C-1), 68.0 (C-3), 60.2 (C-6), 40.1 (NMe_2), 25.4 (CMe_3), 24.2 (Me), 18.4 (CMe_3), −4.6 ($SiMe_2$). MS (electrospray) m/z $[M + H]^+$ 466.3. Accurate mass calcd for $C_{23}H_{36}O_7NSi$: 466.2256: Found 466.2253.

2-*O*-*tert*-Butyldimethylsilyl-4-*O*-[4-(dimethylamino)benzoyl]-6-*O*-pyrenoyl-*myo*-inositol-1,3,5-orthoacetate (10). DCC (0.30 g, 1.5 mmol) and DMAP (0.06 g, 0.13 mmol) were added to a stirred solution of pyrene-1-carboxylic acid (0.37 g, 1.5 mmol) in dry DCM (20 mL) under nitrogen. 2-*O*-*tert*-Butyldimethylsilyl-4-*O*-[4-(dimethylamino)benzoyl]-*myo*-inositol-1,3,5-orthoacetate (**9**) (0.6 g, 1.3 mmol) was added and the reaction mixture was stirred at room temperature for 24 h. The reaction mass was filtered and the filtrate concentrated under reduced pressure. The residue was purified by flash column chromatography (hexane–EtOAc 3 : 1) to give 0.44 g (50%) of **10**. Mp 202–206 °C. IR ν 3491(O–H), 1710 (C=O) cm^{-1}. ^1H NMR ($CDCl_3$) (assignments using ^1H COSY and ^1H NOESY) δ 8.89 (1H, d, J 9.4 Hz, Pyr H-8), 8.34 (1H, d, J 8.1 Hz, Pyr H-16), 8.24–7.92 (7H, m, Pyr H-9–H-15), 7.15 (2H, d, J 9.3 Hz, Ar H-17), 5.81 (1H, t, J 3.8 Hz, H-6), 5.67 (1H, t, J 3.9 Hz, H-4), 5.30 (2H, d, J 9.1 Hz, Ar H-18), 5.06–5.08 (1H, m, H-5), 4.54–4.56 (1H, m, H-2), 4.49 (1H, t, J 1.8 Hz, H-3), 4.30–4.31 (1H, m, H-1), 2.16 (6H, s, NMe_2 H-19), 1.62 (3H, s, CH_3 H-7), 1.00 (9H, s, Bu^t H-21), 0.215 (6H, s, $SiMe_2$ H-20). ^{13}C NMR ($CDCl_3$) δ 166.4 (Pyr C=O), 165.1 (Ar C=O), 152.1 (Ar C-4), 134.2, 131.0, 130.8, 130.7, 130.3, 129.6, 128.0, 126.9, 126.3, 124.6, 124.4, 123.8, 123.7, 122.8 (Pyr-C), 114.3 (Ar C-3,5), 109.2 (C-7), 73.1 (C-6), 69.6 (C-4), 67.9 (C-5), 66.6 (C-2), 61.1 (C-1,3), 38.9 (NMe_2), 26.1 (CMe_3), 24.4 (Me), 18.6 (CMe_3), −4.6 ($SiMe_2$). MS (electrospray) m/z $[M + H]^+$ 694.1. Anal. calcd for $C_{40}H_{43}NO_8Si$: C, 69.24; H, 6.25; N, 2.02; Found C, 68.85; H, 6.06; N, 1.94%.

4,6-Bis-*O*-pyrenoyl-*myo*-inositol (8). Orthoformate (**6**) (0.5 g, 0.70 mmol) was treated with 80% trifluoroacetic acid (5 mL) and the mixture was stirred at room temperature for 4 h. The reaction mixture was concentrated under reduced pressure. The residue was diluted with toluene (4 × 10 mL). The excess toluene was distilled off under reduced pressure, and the solid was crystallised from hexane to give 0.34 g (82%) of **8**. Mp 272 °C (decomp.); IR ν 3497 (O–H), 1701 (C=O) $cm^{-1;}$ ^1H NMR (DMSO-d_6–D_2O) (assignments using COSY) δ 9.11 (2H, d, J 9.6 Hz, Pyr H-8), 8.66 (2H, d, J 8.1 Hz, Pyr H-16), 8.1–8.4 (14H, m, Pyr H-9–H-15), 5.66 (2H, t, J 9.9 Hz, H-4,6), 4.05–4.07 (1H, m, H-2), 3.86–4.03 (3H, m, H-1,3,5). ^{13}C NMR (DMSO-d_6–D_2O) δ 166.9 (C=O), 133.3, 130.5, 129.8, 129.5, 129.3, 129.0, 128.0, 127.1, 126.6, 126.3, 126.1, 125.0, 124.6, 124.1, 123.7, 123.3 (Pyr-C), 76.4 (C-4,6), 73.2 (C-5), 70.3 (C-2), 69.4 (C-1,3). MS (electrospray) m/z $[M + Na]^+$ 659.0. Accurate mass calcd for $C_{40}H_{28}O_8Na$: 659.1676: Found 659.1673.

4-*O*-[4-(Dimethylamino)benzoyl]-6-*O*-pyrenoyl-*myo*-inositol (11). Orthoacetate (**10**) (0.4 g, 0.60 mmol) was treated with 80% trifluoroacetic acid (4 mL) and the mixture was stirred at room temperature for 4 h. The reaction mixture was made basic by the addition of triethylamine (2 mL) and concentrated under reduced pressure. The residue was diluted with toluene (3 × 5 mL). The excess toluene was distilled off under reduced pressure and the residue was purified by column chromatography (EtOAc–CH_2Cl_2 1 : 1) to give 0.18 g (58%) of (**11**). Mp 232 °C (decom); IR ν 3493 (O-H), 1704 (C=O) cm^{-1}. ^1H NMR (DMSO-d_6/D_2O) (assignments using COSY and NOESY) δ 9.26 (2H, d, J 9.4 Hz, Pyr H-8),

8.70 (1H, d, *J* 8.1 Hz, Pyr H-16), 8.1–8.4 (7H, m, Pyr H-9–H-15), 7.91 (2H, d, *J* 9.2 Hz, Ar H-17), 6.71 (2H, d, *J* 9.2 Hz, Ar H-18), 5.86 (1H, t, *J* 9.8 Hz, H-6), 5.64 (1H, t, *J* 9.7 Hz, H-4), 4.25 (1H, t, *J* 2.5 Hz, H-2), 4.11–3.89 (3H, m, H-1,3,5), 3.03 (6H, s, NMe_2 H-19). ^{13}C NMR (DMDO-d_6–D_2O) δ 167.2 (Pyr C=O), 166.0 (Ar C=O), 153.1 (Ar C-4), 133.3, 131.1, 130.5, 129.8, 129.6, 129.4, 129.1, 128.0, 127.1, 126.8, 126.5, 126.2, 124.9, 124.5, 124.2, 123.7, 123.2 (Pyr-C), 116.6 (Ar C-1), 110.6 (Ar C-3,5), 76.2 (C-6), 74.8 (C-4), 72.9 (C-5), 70.3 (C-2), 69.5 (C-1), 69.4 (C-3). MS (electrospray) *m/z* $[M + H]^+$ 556.2. Accurate mass calcd for $C_{32}H_{30}O_8N$: 556.1966: Found 556.1966. Anal. calcd for $C_{32}H_{29}O_8N.1.25H_2O$: C, 66.47; H, 5.50; N, 2.42; Found C, 66.20; H, 5.30; N, 2.62%.

UV fluorescence studies

Fluorescence emission and excitation spectra were recorded in thermostatted 2 mL quartz cuvettes using a controlled-temperature Cary-Eclipse fluorescence spectrophotometer. Emission and excitation spectra were recorded in phosphate buffer pH 7.4 (0.1 M). The excitation wavelength used was 335 nm. Slit-widths were 10 nm. The automatic shutter-on function was used to minimise photo-bleaching of the sample. UV-visible spectra were recorded in 1 mL quartz cuvettes using a Cary 4000 UV-visible spectrophotometer equipped with a Peltier-thermostatted cuvette holder. pH was measured using a Hanna-instruments HI 9321 microprocessor pH meter, calibrated with standard buffers (Sigma) at 20 °C.

Computational studies

Computational conformational analysis was completed using Sybyl 7.3, Tripos Associates.[20] Starting structures were constrained and energy-minimized using the Tripos[21] force field. Chloroform ($\varepsilon = 4.8$) was used as a solvent and Gasteiger–Huckel charges were applied. The number of iterations was 10 000 and the calculation was terminated when the difference in energy between two conformations was no more than 0.005 kcal mol^{-1}. The next step was simulated annealing with heating to 1000 K for 2000 fs followed by cooling to 0 K for 10 000 fs. The conformations obtained were then minimized again using the above procedure (Tripos force field).

Acknowledgements

We gratefully acknowledge Professor K. T. Douglas for his valuable support and Aisha Rafiq for technical assistance. Manikandan Kadirvel was supported by an ORS award and the School of Pharmacy and Pharmaceutical Sciences. Equipment was provided by a grant from the Wolfson Foundation.

References

1 E. V. Bichenkova, H. E. Savage, A. R. Sardarian and K. T. Douglas, *Biochem. Biophys. Res. Commun.*, 2005, **332**, 956–964.
2 E. V. Bichenkova, A. Sardarian, H. E. Savage, C. Rogert and K. T. Douglas, *Assay Drug Dev. Technol.*, 2005, **3**, 39–46.
3 E. V. Bichenkova, A. Gbaj, L. Walsh, H. E. Savage, C. Rogert, A. R. Sardarian, L. L. Etchells and K. T. Douglas, *Org. Biomol. Chem.*, 2007, **5**, 1039–1051.
4 L. Walsh, A. Gbaj, H. E. Savage, M. C. R. Bacigalupo, E. V. Bichenkova and K. T. Douglas, *J. Biomol. Struct. Dyn.*, 2007, **25**, 219–229.
5 K. Fujimoto, H. Shimizu and M. Inouye, *J. Org. Chem.*, 2004, **69**, 3271–3275.
6 K. Ebata, M. Masuko, H. Ohtani and M. Jibu, *Nucleic Acids Symp. Ser.*, 1995, 187–188.
7 K. Ebata, M. Masuko, H. Ohtani and M. Kashiwasake-Jibu, *Photochem. Photobiol.*, 1995, **62**, 836–839.
8 M. Masuko, H. Ohtani, K. Ebata and A. Shimadzu, *Nucleic Acids Res.*, 1998, **26**, 5409–5416.
9 P. L. Paris, J. M. Langenhan and E. T. Kool, *Nucleic Acids Res.*, 1998, **26**, 3789–3793.
10 H. W. Lee and Y. Kishi, *J. Org. Chem.*, 1985, **50**, 4402–4404.
11 T. Praveen and M. S. Shashidhar, *Carbohydr. Res.*, 2001, **330**, 409–411.
12 M. Kadirvel, E. V. Bichenkova, A. D'Emanuele and S. Freeman, *Chem. Lett.*, 2006, **35**, 868–869.
13 S. J. Angyal, *Carbohydr. Res.*, 2000, **325**, 313–320.
14 B. Neises and W. Steglich, *Angew. Chem., Int. Ed. Engl.*, 1978, **90**, 556–557.
15 G. Hoefle, W. Steglich and H. Vorbrueggen, *Angew. Chem., Int. Ed. Engl.*, 1978, **90**, 602–615.
16 A. Hassner and V. Alexanian, *Tetrahedron Lett.*, 1978, 4475–4478.
17 K. M. Sureshan, M. S. Shashidhar, T. Praveen, R. G. Gonnade and M. M. Bhadbhade, *Carbohydr. Res.*, 2002, **337**, 2399–2410.
18 U. Schlueter, J. Lu and B. Fraser-Reid, *Org. Lett.*, 2003, **5**, 255–257.
19 P. Andersch and M. P. Schneider, *Tetrahedron: Asymmetry*, 1996, **7**, 349–352.
20 K. M. Sureshan, M. S. Shashidhar, T. Praveen and T. Das, *Chem. Rev. (Washington, DC, U. S.)*, 2003, **103**, 4477–4503.
21 A. Hassanzadeh, M. Helliwell and J. Barber, *Org. Biomol. Chem.*, 2006, **4**, 1014–1019.
22 *Sybyl 7.3*, Tripos Associates, St. Louis, MO, 2006.
23 M. Clark, R. D. Cramer III and N. Van Opdenbosch, *J. Comput. Chem.*, 1989, **10**, 982–1012.

